

ACTIVE MEDIA

PACS numbers: 42.62.Fi; 32.80.Bx; 32.80.Rm
DOI: 10.1070/QE2005v035n07ABEH003570

Optical cascade pumping of the $7P_{3/2}$ level in cesium atoms

S.V. Kargapol'tsev, V.L. Velichansky, A.V. Yarovitsky, A.V. Taichenachev, V.I. Yudin

Abstract. **Doppler-free absorption spectra of resonance laser fields are studied upon two-stage excitation of cesium atoms according to the schemes $6S_{1/2} \rightarrow 6P_{3/2} \rightarrow 6D_{5/2}$ and $6S_{1/2} \rightarrow 6P_{3/2} \rightarrow 8S_{1/2}$. The obtained experimental results are in qualitative agreement with the theory. In the case of weak absorption saturation, the width of resonances is mainly determined by two-photon transitions. The efficiencies of the two variants of two-stage excitation of the $7P_{3/2}$ level are compared. The possibility of fabrication of a gas laser operating on the 455-nm $7P_{3/2} \rightarrow 6S_{1/2}$ transition with the optical depopulation of the lower operating level by an additional laser is discussed.**

Keywords: *Doppler-free spectroscopy, two-photon transitions, cascade pumping, gas laser.*

1. Introduction

By now lasers of numerous types emitting in different spectral regions have been developed. However, the number of simple cw lasers emitting in the short-wavelength region of the optical spectrum is still small. Recently diode lasers emitting in the blue spectral region have been created, but the manufacturing technology of these lasers is complicated and their emission covers only a part of the blue region. In this connection nonlinear frequency conversion in crystals, in particular, second harmonic generation (SHG) still remains the most popular method for generating short-wavelength radiation in the optical range. Frequency up-conversion is especially attractive for highly efficient semiconductor lasers. However, the output power of single-mode cw diode lasers is, as a rule, insufficient for efficient SHG, which requires the use of build-up cavities [1]. Such systems are also quite complicated. In this paper, we consider an alternative method for frequency up-conversion in gases.

Most efficient methods for producing inversion use a four-level scheme in which the upper operating level has a relatively long lifetime, while the lower level rapidly decays. Another approach is also possible in which the lower operating level is one of the sublevels of the ground state of the system having the hyperfine structure (Fig. 1a). In this case, the lower level is depopulated due to optical pumping of atoms from one ground-state sublevel to another. The population relaxation time for these levels is very large. Along with the depopulation of the lower level, it is necessary to pump the upper operating level. The principal possibility of using such a scheme in a pulsed regime was demonstrated for the D_2 line of sodium (the depopulation was performed at the D_1 line) [2]. However, in this case the wavelength of generated emission is shorter than the initial wavelength only less than by 1 %. It is appropriate to use such an approach for producing inversion and amplification at the short-wavelength operating transition, when two or more long-wavelength lasers are applied for cascade pumping of atoms to the upper operating level.

To study the problem described above, it is convenient to use alkali metal atoms in which the hyperfine ground-state splitting is much greater than the Doppler width. The most suitable are Rb and Cs atoms. They are well studied, the required vapour densities of these metals are achieved at sufficiently low temperatures and the wavelengths of their resonance transitions lie in the emission range of available semiconductor lasers.

In this paper, we studied excitation of the $7P_{3/2}$ level of cesium (Fig. 1b), which can be used as the upper operating level of the $7P_{3/2} \rightarrow 6S_{1/2}$ laser transition. We considered two excitation methods. The first one (SRS) is cascade $6S_{1/2} \rightarrow 6S_{3/2}$ (852.1 nm), $6P_{3/2} \rightarrow 8S_{1/2}$ (794.7 nm) excitation of the $8S_{1/2}$ level followed by a spontaneous transition to the $7P_{3/2}$ level, and the second one (SPD) is cascade excitation from the $6S_{1/2}$ level to the $6P_{3/2}$ level and then to the $6D_{5/2}$ level (917 nm) followed by the decay of the $6D_{5/2}$ level to lower-lying states, including the $7P_{3/2}$ level (Table 1).

The SPD scheme has the following advantages: (i) the oscillator strength for the second $6P_{3/2} \rightarrow 6D_{5/2}$ stage is 4.5 times greater than that for the $6P_{3/2} \rightarrow 8S_{1/2}$ transition for the SPS scheme; (ii) the $6D_{5/2}$ level decays only to the $7P_{3/2}$ level, whereas the $8S_{1/2}$ level can decay both to the $7P_{3/2}$ and $7P_{1/2}$ levels; (iii) it is possible to use cycling transitions at each of the two excitation stages. To avoid the decay of atoms to the long-lived $F = 3$ state, it is appropriate to use only cycling $F = 4 \rightarrow F' = 5$ and $F' = 5 \rightarrow F'' = 6$ transitions, which is possible in the case of circular polarisation of radiation from both pump lasers. Then, the selection rule $\Delta m = 1$ for the right circular polarisation is valid for the magnetic quantum number. In this case, atoms will pre-

S.V. Kargapol'tsev, V.L. Velichansky, A.V. Yarovitsky P.N. Lebedev Physics Institute, Russian Academy of Sciences, Leninskii prosp. 53, 119991 Moscow, Russia; e-mal: sergka@fsl1.lpi.troitsk.ru, vlvlab@okb.lpi.troitsk.ru, ayarovit@mail.ru;
A.V. Taichenachev, V.I. Yudin Institute of Laser Physics, Siberian Branch, Russian Academy of Sciences, prosp. akad. Lavrent'eva 13, 630090 Novosibirsk, Russia; e-mail: llf@laser.nsc.ru

Received 31 January 2005; revision received 13 May 2005
Kvantovaya Elektronika **35** (7) 591 – 597 (2005)
Translated by M.N. Sapozhnikov

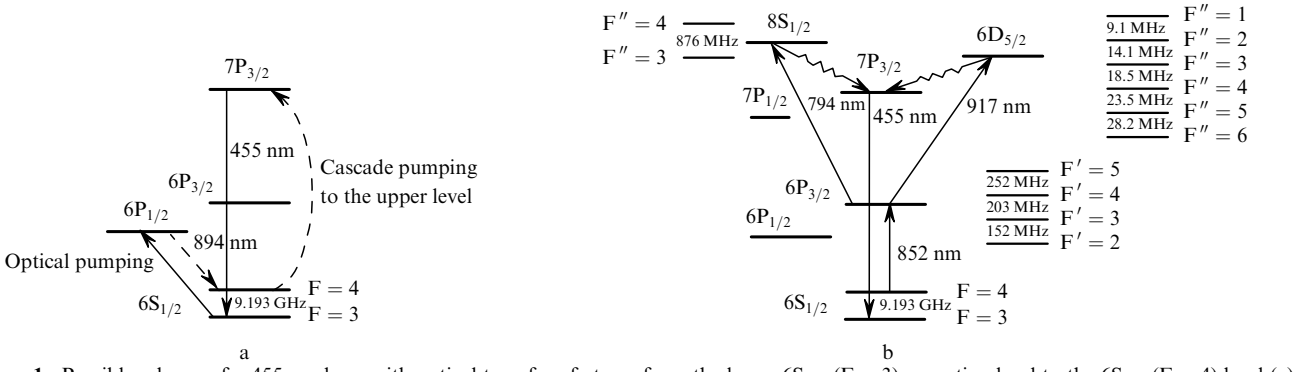

Figure 1. Possible scheme of a 455-nm laser with optical transfer of atoms from the lower $6S_{1/2}$ (F = 3) operating level to the $6S_{1/2}$ (F = 4) level (a) and two possible schemes for optical pumping of atoms to the upper level: $6S_{1/2} \rightarrow 6P_{3/2} \rightarrow 6D_{5/2} \rightarrow 7P_{3/2}$ (SPD scheme) and $6S_{1/2} \rightarrow 6P_{3/2} \rightarrow 8S_{1/2} \rightarrow 7P_{3/2}$ (SPS scheme) (b).

Table 1. Parameters of transitions.

Two-stage pumping scheme	Number of decay cannels from the upper level	Transition	Transition probability/ 10^6 s^{-1}	Branching ratio
SPD	2	$6D_{5/2} \rightarrow 6P_{3/2}$	15.2	0.996
		$6D_{5/2} \rightarrow 7P_{3/2}$	0.063	0.004
SPS	4	$8S_{1/2} \rightarrow 6P_{1/2}$	2.04	0.21
		$8S_{1/2} \rightarrow 6P_{3/2}$	3.60	0.37
		$8S_{1/2} \rightarrow 7P_{1/2}$	1.38	0.14
		$8S_{1/2} \rightarrow 7P_{3/2}$	2.62	0.27

dominantly undergo the $F = 4$ ($m_F = 4$) $\rightarrow F' = 5$ ($m_{F'} = 5$) transition, while at the second stage, transitions from the $F' = 5$ ($m_{F'} = 5$) sublevel can occur only to the $F'' = 6$ ($m_{F''} = 6$) sublevel. The chain of the $F = 4 \rightarrow F' = 5 \rightarrow F'' = 6$ transitions prevents the decay of atoms to the $F = 3$ level upon cascade pumping and simultaneously it is most convenient for populating the upper $6D_{5/2}$ state. However, in this case the $6D_{5/2}$ ($F'' = 6$) state can decay via the $7P_{3/2}$ level only according to the scheme $6D_{5/2}$ ($F'' = 6$) $\rightarrow 7P_{3/2}$ ($F'' = 5$) $\rightarrow 6S_{1/2}$ ($F = 4$). This excludes the possibility of using another ground-state hyperfine level for amplification.

The use of a buffer gas is of interest. Indeed, due to mixing in the $7P_{3/2}$ excited state, the transition from the $7P_{3/2}$ state to another hyperfine level ($F = 3$) of the $6S_{1/2}$ state can occur. On the other hand, mixing in multiplets $6P_{3/2}$ and $6D_{5/2}$ violates cyclicity at each stage, making possible, in particular, the decay of atoms to the $6P_{3/2}$ state and their transition to the $6S_{1/2}$ ($F = 3$) state, which requires an increase in the power of a laser depopulating the $F = 3$ level.

The advantages of the SPS scheme are: (i) a larger branching ratio for the $7P_{3/2}$ level (the relative probability of the $8S_{1/2} \rightarrow 7P_{3/2}$ transition is 27 %, whereas this probability for the $6D_{5/2} \rightarrow 7P_{3/2}$ transition is 0.4 %; the rest of the atoms return back to the $6P_{3/2}$ state); (ii) a simpler hyperfine structure of the upper level, containing only two hyperfine sublevels ($F'' = 3$, 4) separated by 867 MHz, which simplifies selective excitation of the required state [in the case of the SPD scheme, the $6D_{5/2}$ level has six closely spaced hyperfine sublevels (Fig. 1b)].

In this paper, we studied Doppler-free spectra observed upon two-stage excitation at comparatively low intensities and compared the excitation efficiencies of the $7P_{3/2}$ level in the SPS and SPD schemes at high intensities.

2. Theory. Doppler-free spectra upon cascade SPD excitation and the estimate of resonance widths

Hereafter, we will call laser 1 the laser exciting the lower $6S_{1/2} \rightarrow 6P_{3/2}$ transition and laser 2 the laser exciting the upper $6P_{3/2} \rightarrow 8S_{1/2}$ or $6P_{3/2} \rightarrow 6D_{5/2}$ transition. Let us determine the velocity groups of atoms involved in the two-stage $6S_{1/2} \rightarrow 6P_{3/2} \rightarrow 6D_{5/2}$ excitation (Fig. 1b), when excitation is performed in the overlapped counterpropagating beams from both lasers in the Cs atom vapour. Let the frequency ω_2 of laser 2 be varied near the $6P_{3/2} \rightarrow 6D_{5/2}$ transition, while the frequency ω_1 of laser 1 be fixed in the vicinity of the $6S_{1/2}$ ($F = 4$) $\rightarrow 6P_{3/2}$ ($F' = 3$, 4, 5) transitions. Then, in the space of velocity projections of atoms on the propagation direction of laser beams there are three groups of atoms interacting with laser 1 at the $F = 4 \rightarrow F' = 3$, 4, 5 transitions. The excitation rate in these groups depends on the detuning of laser 1 from the frequencies $\omega_{4 \rightarrow F'}$ of atomic transitions and their probability, while the corresponding velocity projections $V_{F'}$ of atoms are determined by the Doppler shift

$$V_{F'} = \frac{\omega_1 - \omega_{4 \rightarrow F'}}{k_1} \qquad (F' = 3, 4, 5), \tag{1}$$

where k_1 is the wave number of the first laser radiation.

Upon tuning the frequency of the counterpropagating wave from laser 2, absorption occurs at the three $F' \rightarrow F''$ transitions ($F'' = F'$, $F' \pm 1$) in each of the groups of atoms, where the $F' = 3$, 4, 5 sublevels of the $6P_{3/2}$ state are populated by laser 1. Taking (1) into account, the frequencies of laser 2 at which these transitions occur are determined by the relation

$$\omega_2^{F' \rightarrow F''} = \omega_{F' \rightarrow F''} - k_2 V_{F'} = \omega_{F' \rightarrow F''} - \frac{k_2}{k_1}(\omega_1 - \omega_{4 \rightarrow F'}), \tag{2}$$

where $\omega_{F' \rightarrow F''}$ are the frequencies of atomic transitions from the sublevels F' of the $6P_{3/2}$ state to the hyperfine sublevels of the $6D_{5/2}$state and k_2 is the wave number of radiation from laser 2. It is easy to obtain from (2) the intervals between Doppler-free resonances of absorption of laser 2 radiation, measured with respect to the $F' = 5 \rightarrow F'' = 6$ transition resonance:

$$\omega_2^{F'\to F''} - \omega_2^{5\to 6} = \delta_{F'\to 6} + \Delta_{F'\to 5}\left(1 - \frac{k_2}{k_1}\right)$$

$$= \delta_{F'\to 6} + \Delta_{F'\to 5}\left(1 - \frac{\lambda_1}{\lambda_2}\right), \quad (3)$$

where $\delta_{F'\to 6}$ are the hyperfine splittings of the $6D_{5/2}$ state measured from the $F'' = 6$ sublevel; $\Delta_{F'\to 5}$ are the hyperfine splittings in the $6P_{3/2}$ state measured from the $F' = 5$ sublevel ($\Delta_{5\to 5} = 0$, $\Delta_{4\to 5} = 252$ MHz, $\Delta_{3\to 5} = 455$ MHz). It follows from (3) that hyperfine splittings, or the absorption 'spectrum' of laser 2 radiation is independent of the laser 1 frequency. As the detuning of laser 2 from the $F' = 5 \to F'' = 6$ transition frequency increases, the frequency of laser 1 being fixed, resonances appear in sequence at frequencies calculated from (3) (Table 2). The obtained intervals correspond to those observed experimentally, which allows the unambiguous interpretation of resonances. Because the fields of the two lasers are counterpropagating, the hyperfine splittings of the $6P_{3/2}$ level in (3) are multiplied by $1 - \lambda_1/\lambda_2 \simeq 0.071$, so that the entire spectrum lies in the interval of width ~ 120 MHz. This also affects the order of sequence of resonances.

Table 2. Cascade excitation of hyperfine levels for the detuning of laser 2 from the $F' = 5 \to F'' = 6$ transition frequency calculated from (3) for nine Doppler-free resonances.

F	F′	F″	Frequency detuning of laser 2 relative to the transition frequency $F' = 5 \to F'' = 6$/MHz
4	5	6	0
4	5	5	28.2
4	4	5	46.1
4	5	4	51.6
4	4	4	69.5
4	3	4	83.9
4	4	3	88.5
4	3	3	102.9
4	3	2	117.3

We calculated the spectra of laser 2 radiation absorption for the three-level system under study. The system is described by the density matrix equation taking into account the hyperfine and Zeeman energy level structures. The relaxation of excited levels was assumed purely radiative, collision effects being neglected, while the ground-state relaxation was determined by the time of flight of atoms through laser beams. The perturbation theory was used in the limit of small saturation parameters for the fields of lasers 1 and 2, respectively:

$$S_1 = \frac{\Omega_{PS}^2}{\gamma_P^2} \ll 1,$$

$$S_2 = \frac{\Omega_{DP}^2}{(\gamma_P + \gamma_D)^2} \ll 1.$$

Here, Ω_{PS} is the Rabi frequency for the lower transition; Ω_{PD} is the Rabi frequency for the upper transition; and $\gamma_P = 5.3$ MHz and $\gamma_D = 2.4$ MHz are the radiative widths of the levels P and D, respectively. By calculating the Doppler-free intensity transmission signal for the field of laser 2, we took into account only the first nonlinear term, proportional to $S_1 S_2$. This term, in turn, consists of two terms, of which the first one (one-photon contribution) is caused by the velocity-selective population of the P state produced by laser 1, and its spectrum has the width [3]

$$\left|\frac{k_2}{k_1}\right|\gamma_{SP} + \gamma_{PD} = 12.6 \text{ MHz}, \quad (4)$$

where $\gamma_{SP} = \gamma_S + \gamma_P = 5.3$ MHz and $\gamma_{PD} = \gamma_P + \gamma_D = 7.7$ MHz. The second term (two-photon contribution) is caused by the S–P coherence and its spectrum has the width

$$\left|\frac{k_2}{k_1}\right|\gamma_{SD} + \left(1 - \left|\frac{k_2}{k_1}\right|\right)\gamma_{PD} \approx 2.8 \text{ MHz}. \quad (5)$$

The redistribution of atoms among Zeeman sublevels in the ground state (optical pumping) is neglected in this order of the perturbation theory. This redistribution is described by higher nonlinearities, beginning with the term $\sim S_1^2 S_2$. Our calculations show that the contribution of two-photon transition dominates and determines the amplitudes and widths of resonances. Figure 2 shows the theoretical spectra for one-photon and two-photon contributions and their sum to absorption of radiation from laser 2 at the $6P_{3/2} \to 6D_{5/2}$ transition.

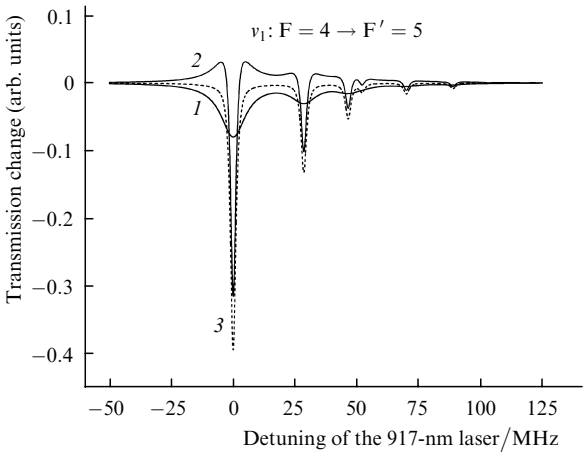

Figure 2. Theoretical one-photon (1) and two-photon (2) absorption spectra of laser 2 at the $6P_{3/2} \to 6D_{5/2}$ transition. Curve (*3*) is the sum of curves (*1*) and (*2*).

3. Experiment

Setup. We used external-cavity single-frequency tunable diode lasers in experiments. At the first stage, a 852-nm laser was employed in both excitation schemes. At the second stage in the SPD scheme, laser 2 was tuned to the $6P_{3/2} \to 6D_{5/2}$ (917 nm) transition frequency, and in the SPS scheme – to the $6P_{3/2} \to 8S_{1/2}$ (794 nm) transition frequency. Different diode lasers were used in the SPS and SPD schemes. The laser beams were directed from opposite sides to a 5.5-cm cell with the ^{133}Cs vapour (Fig. 3). In this case, a greater number of atoms interact with both pump fields than in the case of co-propagating waves [4]. The laser beams overlapped in the region of diameter 3 mm. Photodiodes PD1 and PD2 detected absorption of laser beams propagated through the cell. The fluorescence signal at 455 nm was measured with a FEU-100 photomultiplier.

The hyperfine level in the ground state was depopulated by irradiating the cell by a third laser (not shown in the scheme) tuned to the $6S_{1/2}$ $(F = 3) \rightarrow 6P_{3/2}$ $(F = 4)$ transition. To increase the concentration of atoms, the cell was placed into a heater. The laboratory magnetic field was compensated with Helmholtz coils. The frequency of tunable laser 1 was controlled with the help of a scheme for observing Doppler-free absorption saturation resonances of Cs in an additional cell.

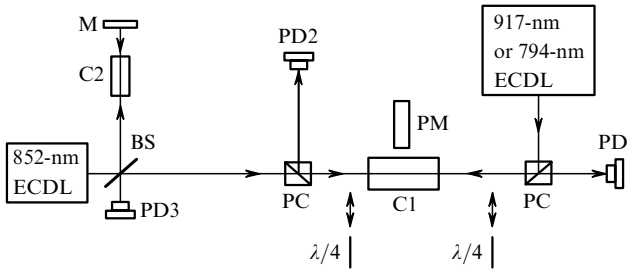

Figure 3. Scheme of the setup: ECDL: external-cavity diode laser; PC: polarisation cube; PM: photomultiplier; C1, C2: cells with the Cs vapour; M: highly reflecting mirror; BS: beamsplitter; PD1–PD3: photodetectors.

Transmission spectra observed in the SPD stage. Figure 4 presents the dependences of absorption of lasers 1 and 2 near the $6P_{3/2} \rightarrow 6D_{5/2}$ transition frequency. Laser 1 was tuned to the $6S_{1/2}$ $(F = 4) \rightarrow 6P_{3/2}$ $(F' = 5)$ transition and its frequency was fixed. The polarisations of laser beams were linear and mutually perpendicular. The observed absorption resonances correspond to the transitions between the hyperfine sublevels of the $6P_{3/2}$ and $6D_{5/2}$ levels.

When laser 1 is tuned to the $F = 4 \rightarrow F' = 4$ transition (Fig. 5), the transmission spectrum has a richer structure. In this case, the resonances corresponding to cycling transitions become weaker, but new resonances appear, which are related to the lower sublevels F' and F''.

All the nine resonances (Table 2) were not always observed. Thus, when laser 1 is tuned to the $6S_{1/2}$ $(F = 4) \rightarrow 6P_{3/2}$ $(F' = 5)$ transition, only five resonances are observed (Fig. 4). The rest of the resonances in Fig. 4 are not observed because of weaker absorption at the $F = 4 \rightarrow F' = 4$ $(4 \rightarrow 4')$ and $F = 4 \rightarrow F' = 3$ $(4 \rightarrow 3')$ transitions, which is caused both by a considerable detuning and lower oscillator strengths of these transitions compared to the oscillator strength for the $4 \rightarrow 5'$ cycling transition. When laser 1 is tuned to the $4 \rightarrow 4'$ transition, all the nine resonances are observed (Fig. 5) because a greater number of atoms populate the $F' = 4$, 3 level, and therefore absorption at the $4' \rightarrow 3''$, $4''$, $5''$, and $3' \rightarrow 2''$, $3''$, $4''$ transitions increases. In this case, absorption at the $5' \rightarrow 6''$, $5''$, $4''$ transitions decreases due to detuning.

The resonances in Figs 4 and 5 can be identified by the absolute values of intervals between them. These intervals coincide within the experimental error with the data presented in Table 2. The lower-frequency resonance appears when a group of atoms resonantly interacting with radiation from laser 1 at the $4 \rightarrow 5'$ transition begins to absorb radiation at the $5' \rightarrow 6''$ transition of the second stage. This is the most intense absorption component for the $6P_{3/2} \rightarrow 6D_{5/2}$ transition, so that absorption of laser 2

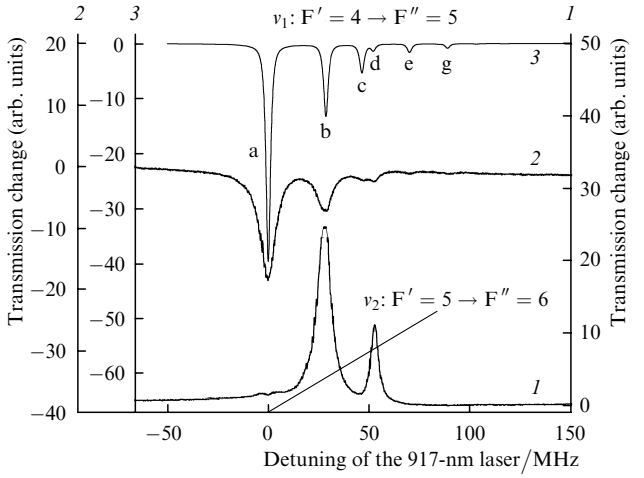

Figure 4. Change in the transmission of radiation of lasers 1 (*1*) and (*2*) as a function of the detuning of laser 2 from the $6P_{3/2}$ $(F' = 5) \rightarrow 6D_{5/2}$ $(F'' = 6)$ transition frequency for the intensity $I_{917\,nm} = 35$ mW cm^{-2} and $I_{852\,nm} = 2$ mW cm^{-2}. The frequency of laser 1 is equal to the $6S_{1/2}$ $(F = 4) \rightarrow 6P_{3/2}$ $(F' = 5)$ transition frequency. Curve (*3*) is the theoretical dependence for laser 2 calculated by the perturbation theory for small saturation parameters. The resonances a, b, c, d, e, and g correspond to the transitions $4 \rightarrow 5' \rightarrow 6''$, $4 \rightarrow 5' \rightarrow 5''$, $4 \rightarrow 4' \rightarrow 5''$, $4 \rightarrow 5' \rightarrow 4''$, $4 \rightarrow 4' \rightarrow 4''$, and $4 \rightarrow 4' \rightarrow 3''$, respectively.

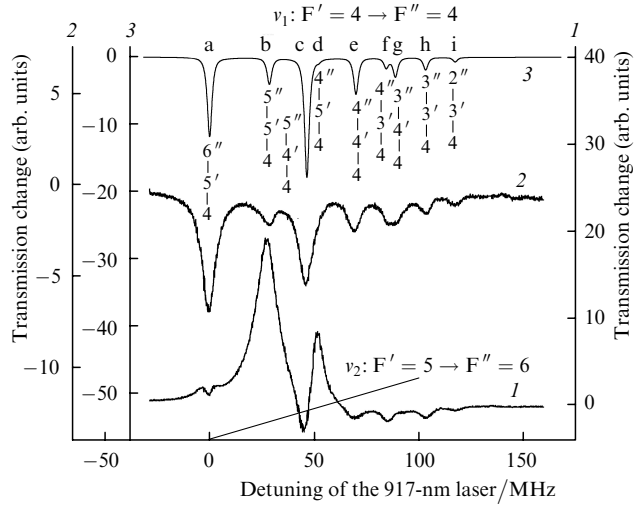

Figure 5. Change in the transmission of radiation of lasers 1 (*1*) and (*2*) as a function of the detuning of laser 2 from the $6P_{3/2}$ $(F' = 5) \rightarrow 6D_{5/2}$ $(F'' = 6)$ transition frequency for the intensity $I_{917\,nm} =$ 35 mW cm^{-2} and $I_{852\,nm} = 2$ mW cm^{-2}. The frequency of laser 1 is equal to the $6S_{1/2}$ $(F = 4) \rightarrow 6P_{3/2}$ $(F' = 4)$ transition frequency. Curve (*3*) is the theoretical dependence for laser 2 calculated by the perturbation theory for small saturation parameters. The resonances f, g, h, and i correspond to the transitions $4 \rightarrow 3' \rightarrow 4''$, $4 \rightarrow 4' \rightarrow 3''$, $4 \rightarrow 3' \rightarrow 3''$, and $4 \rightarrow 3' \rightarrow 2''$, respectively.

radiation is maximal. The b, c, and d resonances are related to the $4 \rightarrow 5' \rightarrow 5''$, $4 \rightarrow 4' \rightarrow 5''$ and $4 \rightarrow 5' \rightarrow 4''$ transitions, respectively. The c and d resonances are closely spaced and almost unresolved in the absorption spectrum for laser 2 radiation [curve (*2*) in Figs 4 and 5]. However, they are resolved in the absorption spectrum for laser 1 radiation because they have different signs [curve (*1*) in Fig. 5]. The e resonance corresponds to the $4 \rightarrow 4' \rightarrow 4''$ transition. The f and g resonances are merged into one and correspond to the $4 \rightarrow 3' \rightarrow 4''$ and $4 \rightarrow 4' \rightarrow 3''$ transi-

tions. The two remaining resonances h and i correspond to the $4 \rightarrow 3' \rightarrow 3''$ and $4 \rightarrow 3' \rightarrow 2''$ transitions, respectively.

The experimental widths of resonances were 5± 0.5 MHz, which is smaller than the width determined by one-photon process (4) but somewhat larger than the width caused by two-photon process (5). Some additional broadening can appear because of the residual angle between the laser beams and due to their divergence. The laser field also broadens the observed resonances. In any case, the experimental widths of resonances in the absorption spectrum for laser 2 radiation show that two-photon processes dominate over one-photon processes, in accordance with the theory.

The intensities of the $4' \rightarrow 5''$, $4''$, $3''$ resonances in the spectra obtained upon large detuning are lower than those predicted by the theory. This is explained by the fact that the theory neglects the redistribution of atoms among Zeeman sublevels in the ground state.

Dependence of the efficiency of excitation of atoms into the $7P_{3/2}$ level on polarisation. We studied the $7P_{3/2}$ level excitation efficiency as a function of the laser radiation polarisation. The dependence of the $7P_{3/2} \rightarrow 6S_{1/2}$ (455 nm) fluorescence on the frequency of circularly polarised radiation from laser 2 was investigated for different polarisations of laser 1 radiation. The frequency of laser 1 was fixed in the vicinity of the $4 \rightarrow 5'$ transition. Because laser 2 was tuned, the fluorescence spectrum exhibits a part of the structure of the $6D_{5/2}$ level. The population efficiency was maximal when radiations of lasers 1 and 2 had the same circular polarisation [curve (*1*) in Fig. 6]. The spectra in Fig. 6 exhibit only peak a, whereas the intensities of other components are small. This is explained by excitation of only two cycling $4 \rightarrow 5'$ and $5 \rightarrow 6''$ transitions. Radiation of laser 1 with polarisation σ^+ populates only the $F' = 5$ ($m_{F'} = 5$) hyperfine sublevel. Therefore, if radiation of laser 2 also has polarisation σ^+, transitions can occur from this sublevel only to the $F'' = 6$ ($m_{F''} = 6$) sublevel, which explains the absence of other peaks in Fig. 6 [curve (*1*)]. In this case, optical pumping to the $F = 3$ level is impossible, and therefore the fluorescence signal is maximal. The splitting of peak a is probably caused by the dynamic Stark effect.

When radiation of laser 1 is linearly polarised, other magnetic sublevels can be populated, resulting in the appearance of new spectral components [curve (*2*) in Fig. 6]. When radiation of laser 1 has circular polarisation, which is orthogonal to the circular polarisation of radiation from laser 2, the population of the $F'' = 6$ sublevel and the blue fluorescence intensity are minimal [curve (*3*) in Fig. 6]), while the leakage of atoms to the $F = 3$ level is maximal.

Elimination of hyperfine optical pumping in the ground state. Irradiation by the third laser tuned to the $6S_{1/2}$ ($F = 3$) $\rightarrow 6P_{3/2}$ ($F = 3$) transition eliminates optical pumping to the $F = 3$ sublevel and enhances the fluorescence intensity. However, this is weakly manifested in the case of the same circular polarisation of radiation from lasers in the SPD scheme because the cyclicity of transitions prevents the transfer of atoms to the $F = 3$ sublevel. The role of the third laser substantially increases in the SPS scheme, where only laser 1 can be tuned to the cycling transition.

Transmission spectra observed in the SPS stage. Similarly to the previous case, for the same geometry and mutual orthogonal linear polarisations of laser beams, we detected

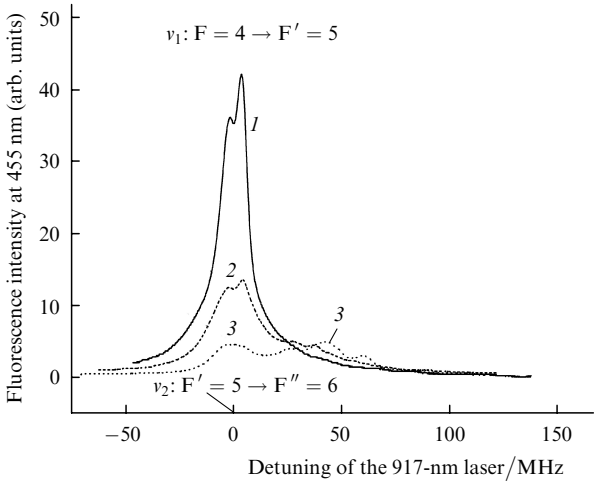

Figure 6. Dependences of the fluorescence intensity at the $7P_{3/2} \rightarrow 6S_{1/2}$ transition on the laser 2 frequency for the σ^+ polarisation of laser 2 radiation and the σ^+ (*1*), π (*2*), and σ^- (*3*) polarisations of laser 1 in the $6S_{1/2} \rightarrow 6P_{3/2} \rightarrow 6D_{5/2}$ excitation scheme for the intensity $I_{917\,nm}$ = 30 mW cm^{-2} and $I_{852\,nm}$ = 120 mW cm^{-2}.

the dependences of Doppler-free absorption of laser radiation at 794 and 852 nm on the frequency of the 794-nm laser. Figures 7–10 present the transmission spectra for radiation from lasers 1 and 2 as functions of the detuning of the 794-nm laser. The frequencies of absorption resonances for radiation of laser 2 in the case of counterpropagating beams can be determined as in the SPD scheme using relations similar to (1)–(3). In this scheme, the $8S_{1/2}$ state has two hyperfine sublevels spaced by 876 MHz. Therefore, the structure of absorption spectra is simpler than that in the SPD scheme.

The only allowed transition from the $6P_{3/2}$ ($F' = 5$) level is the transition to the $8S_{1/2}$ ($F'' = 4$) level, and the absorption spectrum for laser radiation exhibits only one resonance a for a group of atoms excited to the $F' = 5$ sublevel (Fig. 7), corresponding to the $5' \rightarrow 4''$ transition. When the laser is tuned to the $4 \rightarrow 5'$ transition, the number of atoms excited to the $4'$ and $3'$ sublevels is small due to the frequency detuning and a lower intensity of the $4 \rightarrow 3'$, $4'$ transitions. As a result, absorption at the $6P_{3/2} \rightarrow 8S_{1/2}$ transition from the $4'$ and $3'$ sublevels is almost absent against the background of absorption from the $5'$ sublevel (Fig. 7). As in the case of the SPD scheme, absorption increases upon tuning laser 1 to the red. When laser 1 is tuned to the $4 \rightarrow 4'$ transition, the $4 \rightarrow 3'$, $4' \rightarrow 3''$, $4''$ transitions become noticeable in the absorption spectrum of laser radiation. These transitions become even more distinct when the laser is tuned to the $4 \rightarrow 3'$ transition, but the $4 \rightarrow 4' \rightarrow 5''$ transition becomes substantially weaker.

Consider in more detail the case when laser 1 is detuned by 450 MHz to the red from the $6S_{1/2}$ ($F = 4$) $\rightarrow$ $6P_{3/2}$ ($F' = 5$) frequency (Fig. 8). In this situation, all possible transitions are observed because all the sublevels of the $6P_{3/2}$ state are relatively uniformly populated due to the tuning of laser to the $4 \rightarrow 3'$ transition, while the $4 \rightarrow 4'$ and $4 \rightarrow 5'$ lines are more intense than the $4 \rightarrow 3'$ line. Figure 9 shows the enlarged fragment of the left part of Fig. 8 corresponding to the $4 \rightarrow 4' \rightarrow 3''$ and $4 \rightarrow 3' \rightarrow 3''$ transitions (peaks d and e, respectively), while Fig. 10 demonstrates the enlarged right part of Fig. 8 corresponding

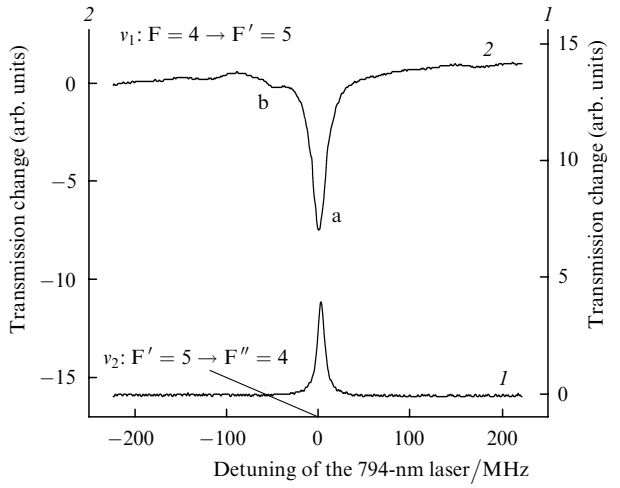

Figure 7. Change in the transmission of lasers 1 (*1*) and (*2*) as a function of the detuning of laser 2 from the $6P_{3/2}$ (F′ = 5) → $8S_{1/2}$ (F″ = 4) transition frequency for the intensity $I_{794\,nm} = 40$ mW cm^{-2} and $I_{852\,nm} = 40$ mW cm^{-2}. The frequency of laser 1 is equal to the $6S_{1/2}$ (F = 4) → $6P_{3/2}$ (F′ = 5) transition frequency. The resonances a and b correspond to the transitions 4 → 5′ → 4″, and 4 → 4′ → 4″, respectively.

to the group of high-frequency resonances related to the 4 → 5′ → 4″, 4 → 4′ → 4″, 4 → 3′ → 4″ transitions (peaks a, b, and c). For laser 2 (Figs 9 and 10), as in the case of the SPD scheme, all the resonances are absorption peaks. In the transmission spectrum of laser 1, transmission resonances corresponding to the 4 → 5′ → 4″ and 4 → 4′ → 3″ transitions are possible, as well as absorption resonances corresponding to the 4 → 3′, 4′ → 4″, and 4 → 3′ → 3″ transitions. By comparing this result with that for the SPD scheme, we see that in the case of linearly polarised laser fields, all the cycling transitions in the absorption spectrum of laser 1 are transmission resonances, while non-cycling transitions are absorption resonances.

Comparison of the SPD and SPS excitation efficiencies. At higher concentrations of the saturated vapour of Cs atoms (of the order of 4×10^{12} cm^{-3}), we measured the power of fluorescence at 455 nm in a 3.5-cm cell, where the fluorescence region was localised to increase the geometrical factor of emission collection. The cell was heated up to 60 °C. Absorption at the $6P_{3/2} \rightarrow 8S_{1/2}$ transition in the SPS scheme was 45 %. Estimates made from the transition probabilities [5] show that only 14% of photons absorbed upon this transition contribute to the detected fluorescence. Upon excitation of the upper stage $6P_{3/2} \rightarrow 8S_{1/2}$ transition

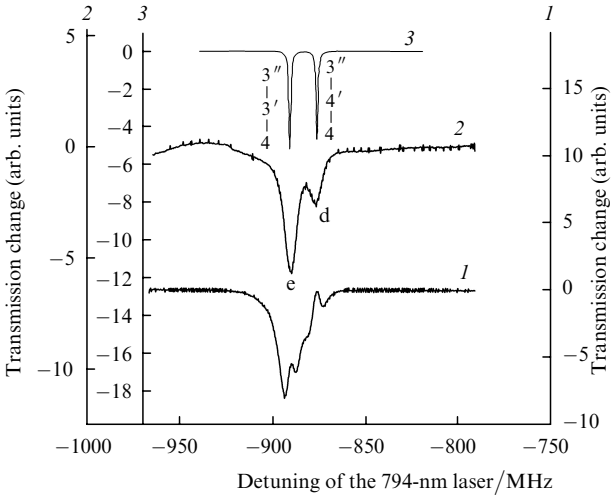

Figure 9. Fragment of the left part of Fig. 8. Curve (*3*) is the theoretical dependence for laser 2 calculated by the perturbation theory for small saturation parameters. The resonances d and e correspond to the transitions 4 → 4′ → 3″, and 4 → 3′ → 3″, respectively. The intensities are $I_{794\,nm} = 55$ mW cm^{-2} and $I_{852\,nm} = 10$ mW cm^{-2}.

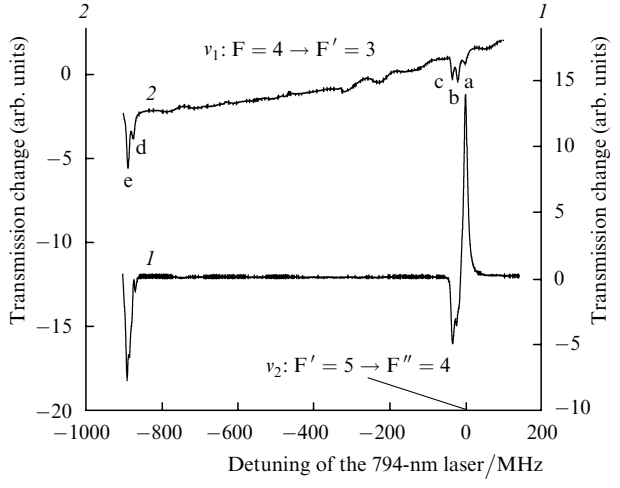

Figure 8. Change in the transmission of lasers 1 (*1*) and (*2*) as a function of the detuning of laser 2 from the $6P_{3/2}$ (F′ = 5) → $8S_{1/2}$ (F″ = 4) transition frequency for the intensity $I_{794\,nm} = 55$ mW cm^{-2} and $I_{852\,nm} = 10$ mW cm^{-2}. The frequency of laser 1 is reesonant to the $6S_{1/2}$ (F = 4) → $6P_{3/2}$ (F′ = 3) transition. The resonances a, b, c, d, and e correspond to the transitions 4 → 5′ → 4″, 4 → 4′ → 4″, 4 → 3′ → 4″, 4 → 4′ → 3″, and 4 → 3′ → 3″, respectively.

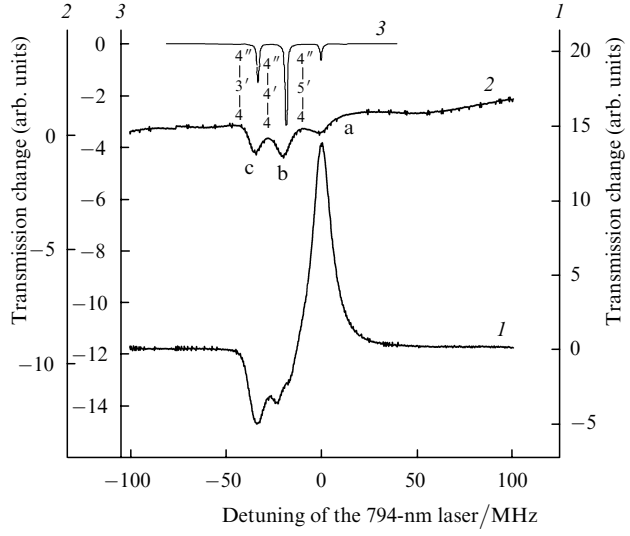

Figure 10. Fragment of the right part of Fig. 8. Curve (*3*) is the theoretical dependence for laser 2 calculated by the perturbation theory for small saturation parameters. The resonances a, b, and c correspond to the transitions 4 → 5′ → 4″, 4 → 4′ → 4″, and 4 → 3′ → 4″, respectively. The intensities are $I_{794\,nm} = 55$ mW cm^{-2} and $I_{852\,nm} = 10$ mW cm^{-2}.

in the cell by laser radiation of power 3.6 mW, the power of blue fluorescence is $k \times 0.45 \times 0.14 \times 3.6$ mW ≈ 400 μW, where $k = 794$ nm/455 nm is a coefficient taking into account different photon energies. The power of fluorescence at 455 nm measured in the experiment was 300 μW, which, taking into account the error in the calculation of the geometrical factor of fluorescence collection, is in agreement with the theoretical estimate 400 μW. Under similar conditions, absorption of radiation in the upper $6P_{3/2} \rightarrow 6D_{5/2}$ transition in the SPD scheme was 70 %. Only 0.15 % of these absorbed photons contribute to fluorescence. For the 0.6-mW incident power, the power of fluorescence at 455 nm will be 1.2 μW. The experimental power was 1.1 μW.

4. Conclusions

We have studied Doppler-free absorption spectra of laser radiation in two cascade schemes $6S_{1/2} \rightarrow 6P_{3/2} \rightarrow 6D_{5/2}$ and $6S_{1/2} \rightarrow 6P_{3/2} \rightarrow 8S_{1/2}$ (dependence of the transmission of laser radiation on the frequency of the second-stage laser at the fixed frequency of the first-stage laser). The relations for the frequency intervals between Doppler-free resonances have been obtained and used for identification of resonances. The structure of the spectra coincides qualitatively with the structure calculated for weak fields with intensities lower than the transition saturation intensity. The widths of resonances measured in experiments suggest that two-photon transitions dominate over one-photon transitions in the two-stage process.

Two pump schemes for the $7P_{3/2}$ level are compared: (i) $6S_{1/2} \rightarrow 6P_{3/2} \rightarrow 6D_{5/2}$ followed by the decay of the $6D_{5/2}$ level to the $7P_{3/2}$ level (SPD scheme) and (ii) $6S_{1/2} \rightarrow 6P_{3/2} \rightarrow 8S_{1/2}$ followed by the spontaneous transition to the $7P_{3/2}$ level (SPS scheme). The SPS scheme is preferable for the efficient excitation of the $7P_{3/2}$ level because weaker absorption of radiation at the $6P_{3/2} \rightarrow 8S_{1/2}$ transition and a greater number of decay channels in this scheme are well compensated by a large branching ratio to the upper $7P_{3/2}$ level. Optical pumping by an additional laser can prevent the transfer of atoms to the $F = 3$ level, thereby increasing the excitation efficiency of the $7P_{3/2}$ level. Note that the presence of additional (depopulating) radiation (Fig. 1a) under certain conditions can switch on the inversionless amplification mechanism, which appears in the V scheme upon the absorption-destructive interference of the excitation probability amplitudes of atoms [6, 7]. This contribution will be sensitive to the linewidth of depopulating radiation.

Acknowledgements. This work was supported by the ISTC (Grant No. 265r) and the Russian Foundation for Basic Research (Grant Nos 05-02-17086 and 04-02-16488).

References

1. Goldberg L., Chun M.K. *Appl. Phys. Lett.*, **55**, 218 (1989).
2. Apolonsky A.A., Babin S.A., et al. *Phys. Rev. A*, **61**, 033408 (2000).
3. Frish S.E. *Opticheskie spektry atomov* (Optical Spectra of Atoms) (Moscow: Izd. Fiz. Mat. Lit., 1963).
4. Cagnac B. *Kvantovaya Elektron.*, **5**, 1651 (1978) [*Sov. J. Quantum. Elektron.*, **8**, 949 (1978)].
5. Heavens O.S. *J. Opt. Soc. Am.*, **51**, 1058 (1961).
6. Mandel P. *Contemporary Phys.*, **14**, 235 (1993).
7. Scully M.O., Zubairy M.S. *Quantum Optics* (Cambridge: University Press, 1998).